Impact of Profilin on Actin-Bound Nucleotide Exchange and Actin Polymerization Dynamics[†,‡]

Lynn A. Selden,[§] Henry J. Kinosian,[||] James E. Estes,*[,§,||] and Lewis C. Gershman[§,||,⊥]

Research Service and Medical Service, Stratton VA Medical Center, Albany, New York 12208, and Department of Physiology & Cell Biology and Department of Medicine, Albany Medical College, Albany, New York 12208

Received June 29, 1998; Revised Manuscript Received January 8, 1999

ABSTRACT: We have investigated the effects of profilin on nucleotide binding to actin and on steady state actin polymerization. The rate constants for the dissociation of ATP and ADP from monomeric Mg−actin at physiological conditions are 0.003 and 0.009 s^{-1}, respectively. Profilin increases these dissociation rate constants to 0.08 s^{-1} for MgATP−actin and 1.4 s^{-1} for MgADP−actin. Thus, profilin can increase the rate of exchange of actin-bound ADP for ATP by 140-fold. The affinity of profilin for monomeric actin is found to be similar for MgATP−actin and MgADP−actin. Continuous sonication was used to allow study of solutions having sustained high filament end concentrations. During sonication at steady state, F-actin depolymerizes toward the critical concentration of ADP−actin [Pantaloni, D., et al. (1984) *J. Biol. Chem. 259*, 6274−6283], our analysis indicates that under these conditions a significant number of filaments contain terminal ADP−actin subunits. Addition of profilin to this system increases the polymer concentration and increases the steady state ATPase activity during sonication. These data are explained by the fast exchange of ATP for ADP on the profilin−ADP−actin complex, resulting in rapid ATP−actin regeneration. An important function of profilin may be to provide the growing ends of filaments with ATP−actin during periods when the monomer cycling rate exceeds the intrinsic nucleotide exchange rate of monomeric actin.

The central role of actin polymerization in cellular motile activity is apparent in a variety of processes, such as the protrusion of lamellipodia during locomotion or shape changes of living cells (*1*, *2*), as well as in the propulsive movement of the pathogenic bacteria *Listeria monocytogenes* (*3*). The steady state assembly of F-actin in solutions containing excess ATP results in a continuous cycling of monomeric actin with the concomitant hydrolysis of actin-bound ATP. As the filament number increases, the cycling rate increases. Since nucleotide exchange occurs primarily on monomeric actin, the rate of regeneration of ATP−actin[1] is limited by the release of ADP from newly dissociated monomers. At high filament concentrations, the rate of release of ADP−actin from the polymer ends can exceed the rate at which ATP−actin can be regenerated, causing a rise in the free monomer concentration toward the critical concentration of ADP−actin (*4*), 10−15-fold higher than the critical concentration of ATP−actin.

Profilin is a small actin-binding protein that is known to bind tightly to monomeric actin. Profilin has been shown to promote the polymerization of actin at the barbed ends of filaments (*5*), but not at the pointed ends. This function of profilin has important implications for actin filament dynamics. When barbed ends of filaments are capped, profilin functions as a G-actin sequestering protein. When barbed ends become uncapped, profilin−actin complexes add onto the free barbed ends and profilin is released from the complex.

One consequence of profilin binding to monomeric actin is a reduction in the affinity of nucleotide for actin (*6*, *7*). Goldschmidt-Clermont et al. (*6*) were the first to propose that the regulation of nucleotide exchange on actin is a potential mechanism by which cells regulate the monomeric actin pool. Perelroizen et al. (*7*) reported a 20-fold higher affinity of profilin for ϵATP−actin than for ϵADP−actin and a rate constant of 0.2 s^{-1} for the dissociation of MgϵADP from MgϵADP−actin in the absence of profilin. A rate of exchange of this magnitude would mean that monomeric MgADP−actin could become recharged with ATP at a relatively fast rate. Therefore, it was argued that the increase

[†] This work was supported by Department of Veterans Affairs Grant 0398-002 (L.C.G.) and National Institutes of Health Grant GM 32007 (J.E.E.).

[‡] Presented at the 37th Annual American Society for Cell Biology meeting; abstract published in 1997 (*Mol. Biol. Cell 8,* 255a).

* To whom correspondence should be addressed: Research Service (151), Stratton VA Medical Center, 113 Holland Ave., Albany, NY 12208. Phone: (518) 462-3311, ext 2213. Fax: (518) 462-0626. E-mail: estes.james_e@albany.va.gov.

[§] Research Service, Stratton VA Medical Center.

[||] Department of Physiology & Cell Biology, Albany Medical College.

[⊥] Medical Service, Stratton VA Medical Center, and Department of Medicine, Albany Medical College.

[1] Abbreviations: MgATP−actin (G_T) and MgADP−actin (G_D), monomeric (G) actin which contains bound MgATP and MgADP, respectively, at the high-affinity site; ϵATP, 1,N^6-ethenoadenosine 5′-triphosphate; ϵADP, 1,N^6-ethenoadenosine 5′-diphosphate; MESG, 2-amino-6-mercapto-7-methylpurine ribonucleoside; PNP, purine nucleoside phosphorylase; EGTA, ethylene glycol bis(β-aminoethyl ether)-*N*,*N*,*N*′,*N*′-tetraacetic acid; MOPS, 3-(morpholino)propanesulfonic acid.

10.1021/bi981543c CCC: $18.00
Published on Web 02/11/1999

in the rate of nucleotide exchange on actin, induced by profilin, is not important to its physiological function (*7*). In subsequent work supporting this hypothesis, it was reported that plant profilin does not enhance nucleotide exchange on skeletal muscle actin, but functions in a manner similar to that of mammalian profilin in other respects (*8*).

The differences between the results of Perelroizen et al. (*7*) and the nucleotide exchange rates predicted from our previous work (*9*, *10*) stimulated the present study. In the study described here, we directly determine the dissociation rate constants for MgADP−actin and MgATP−actin at physiological ionic strength in the presence and absence of profilin. We find that the rate constants for nucleotide exchange in the absence of profilin are much slower than those reported by Perelroizen et al. (*7*) and are in agreement with those we had predicted (*9*, *10*). The differences may be due to the weaker binding of ϵADP and ϵATP, at the higher than physiological pH (8.0) in their study.

Our experiments show that profilin increases the rate of exchange of ϵATP for actin-bound nucleotide by 140-fold for MgADP−actin, but only 25-fold for MgATP−actin. Profilin binds with similar affinities to MgADP− and MgATP−actin; the result is a rapid shift in the nucleotide binding, favoring MgATP−actin. From measurements of actin polymerization during sonication, we find a significant increase in the actin monomer concentration as a function of the filament number concentration in the absence of profilin. Experiments on the effects of profilin during sonication of F-actin solutions show that profilin increases the F-actin concentration and increases ATP hydrolysis rates. Our results suggest that slow nucleotide exchange is a rate-limiting step in the cycling of ATP−actin monomers in F-actin solutions containing high filament number concentrations; elimination of this slow kinetic step may be an important function of profilin.

MATERIALS AND METHODS

Protein Preparations. Actin was isolated from skeletal muscle acetone powder as previously described (*11*). Profilin was prepared from calf spleen using a poly(L-proline) column prepared as described by Lindberg et al. (*12*). The procedure of Lindberg et al. (*12*) was followed for tissue homogenization, column application, and washing. Elution was accomplished by the method of Kaiser et al. (*13*), in which 4 M urea was used to remove any actin and profilin−actin complexes from the column. Profilin was then eluted with 8 M urea and renatured by dialysis against 5 mM Tris and 0.5 mM DTT (pH 7.4). To concentrate the profilin, the pH was lowered to 6.0 by addition of the acid form of MOPS, and the protein was applied to a 0.7 cm × 2 cm CM-Sepharose FF column equilibrated with the same pH 6.0 buffer. Profilin was retained on this column, and after the column was washed thoroughly with buffer, profilin was eluted with 0.5 M KCl. The protein was then dialyzed against 5 mM Tris (pH 7.4) and 0.5 mM DTT to remove the salt.

Nucleotide Exchange Experiments. Experiments were carried out in buffer containing 10 mM MOPS, 0.1 M KCl, and 2 mM $MgCl_2$ (pH 7.0) (buffer X). In all cases, the actin initially contained ATP or ADP as the bound nucleotide. Exchange was initiated by addition of a molar excess of ϵATP. In experiments in which bound ATP was replaced, 20−30 μM actin was passed through a 1 cm × 8 cm column of Spherulose 90 (ISCO) equilibrated with 10 mM MOPS (pH 7.0). The pooled actin peak (4−6 μM) was checked for nucleotide content by observing the OD at 280 and 260 nm. A typical 280:260 ratio of 1.5 was obtained, indicating that the actin contained very little free ATP. The actin was briefly incubated with 100 μM $MgCl_2$ and 100 μM EGTA on ice for 5 min before dilution to 0.5 μM in buffer X containing ϵATP. Experiments in which the ϵATP concentration was varied to ensure that competition between free ATP and ϵATP was negligible showed that at 0.2−0.5 μM MgATP−actin, 10 μM ϵATP was adequate to ensure noncompetitive exchange of ϵATP for ATP. Exchange of ϵATP into MgADP−actin was accomplished by first preparing 25−30 μM MgADP−actin at pH 8.0 as previously described (*14*). This MgADP−actin was then diluted to 0.2−0.5 μM into buffer X containing 20 μM ϵATP. In this case, the free ADP concentration was 3−5 μM and, as was shown by Kinosian et al. (*9*), ϵATP replaces ADP in a noncompetitive reaction at ϵATP:ADP concentration ratios of >1.0. Excitation and emission wavelengths of 340 and 460 nm, respectively, were used to monitor ϵATP fluorescence intensity in an SLM-Aminco AB2 spectrofluorimeter. All reactions were accomplished using a stirred cuvette containing ϵATP to which a sample of actin was added through a small opening in the top of the sample compartment while the fluorescence intensity was being recorded. Observed rate constants, k_{obs}, were determined from the exponential fluorescence intensity increase on binding of ϵATP (*9*).

Polymerization Experiments. The intrinsic tryptophan fluorescence of actin was used to monitor actin polymerization using excitation and emission wavelengths of 300 and 335 nm, respectively (*15*). To quantitatively measure F-actin due to fluorescence changes by this method, the fluorescence intensities of free profilin and the profilin−actin complex must be considered. We determined the relative fluorescence intensities for the MgATP−actin monomer, the Mg−actin polymer, free profilin, and the profilin−actin complex to be 1, 0.7, 0.13, and 0.9, respectively, in good agreement with the literature (*15*, *16*). Note that the fluorescence intensity of the profilin−actin complex is 20% smaller than the sum of fluorescence intensities of the free actin monomer and free profilin, reflecting tryptophan fluorescence quenching within the profilin−actin complex (*16*). Using these relative fluorescence values, one can calculate that the relative fluorescence intensity decrease resulting from polymerization of the profilin−actin complex is ∼8%. Throughout this work, we have minimized the fluorescence contributions of free profilin and the profilin−actin complex by keeping the concentration of profilin low. In the experiments whose results are depicted in Figures 4 and 5, where the profilin concentration was ≤0.1 μM, profilin has a negligible effect on the fluorescence intensity of the data and the F-actin concentration was calculated from a standard curve (critical concentration plot) without profilin. The data of Figure 6 were collected from three independent experiments, each of which included critical concentration plots with and without 0.5 μM profilin for conversion of fluorescence to F-actin concentration (i.e., critical concentration plots in Figure 3A). In a typical polymerization experiment, CaATP−actin was mixed with buffer X in a cuvette and the mixture incubated at a high Mg^{2+}:Ca^{2+} ratio to form MgATP−actin, during which time a small amount of polymer formed. The

incubation time was varied depending on the actin concentration so that the amount of polymer formed was negligible as determined by the fluorescence intensity change, but was enough so that fragmentation upon sonication produced F-actin "seeds" to induce rapid polymerization. While fluorescence intensity was being measured, sonication at 7 W was applied with the 2 mm tip of an ultrasonic homogenizer (Cole Parmer Instrument Co., Chicago, IL) introduced through the top of the sample compartment. On cessation of sonication, samples achieved the same polymerization plateau as a control sample that had not undergone sonication, indicating that no significant denaturation occurred during the time frame of the experiments. The results of the fluorescence intensity experiments were verified by a series of light scattering experiments (as in Figure 8A) over a concentration range of 1−4 μM actin. In general, the noise during sonication was too troublesome for routine light scattering measurements.

Determination of the Filament Number during Sonication. The number of filaments generated at steady state during sonication was determined by removing a 0.15 mL aliquot of a sample under sonication and immediately adding it to a 1.5 mL sample of 2 μM MgATP−actin in the presence of 0.1 M KCl, 2 mM $MgCl_2$, 2 mM Tris, 0.2 mM ATP, 0.02 mM $CaCl_2$, and 0.1 mM EGTA (pH 7.3). The aliquot was transferred within 2 s using a pipet tip with the end cut off to widen the orifice. The polymerization curve was fit by an exponential in which the filament number, [m], was calculated as

$$[\mathrm{m}] = k_{\mathrm{obs}}/k_{+}$$

where k_+ (12 μM^{-1} s^{-1}) is the elongation rate constant for addition of the MgATP−actin monomer to polymer ends (*17*) and k_{obs} is the observed rate constant of the exponential increase in polymer. The rate constant measured in the absence of added filament ends (<0.001 s^{-1}) was about $^1/_{10}$ of the slowest rate measured in the presence of added filament ends. Under conditions when spontaneous nucleation is slow, polymerization of the monomer onto the ends of the added polymer acts to progressively decrease the rate of spontaneous nucleation; therefore, we neglected the small contribution from spontaneous nucleation.

Release of Phosphate from the Actin Polymer. Inorganic phosphate (P_i) was monitored using MESG, a P_i indicator developed by Webb (*18*), which increases in absorbance at 360 nm upon enzymatic conversion to ribose 1-phosphate and 2-amino-6-mercapto-7-methylpurine by PNP. This indicator and enzyme were purchased as an Enz Check Phosphate Assay Kit (Molecular Probes, Inc., Eugene, OR). MESG was stored frozen in 200 μL aliquots at a concentration of 1 mM. A stock solution of 1000 units/mL PNP was stored at 5 °C. Fluorescence and absorbance measurements were taken using an SLM-Aminco AB2 spectrofluorimeter fitted with an additional photomultiplier to detect the excitation light transmitted through the cuvette. Actin samples (1−4 μM) were prepared in 20 mM MOPS (pH 7.0), 0.04 mM ATP, 0.03 mM MESG, and 2 units/mL PNP (3 mL final volume). Polymerization was started by addition of 0.1 M KCl and 2 mM $MgCl_2$ during sonication as described above, and P_i release was monitored as the increase in absorption at 360 nm. In control experiments using MESG without PNP, a minimal change in the absorbance of MESG equivalent to <0.5 μM P_i was noted on polymerization of 5 μM MgATP−actin. This increase can most likely be attributed to light scattering. We did not correct for this effect in the data presented.

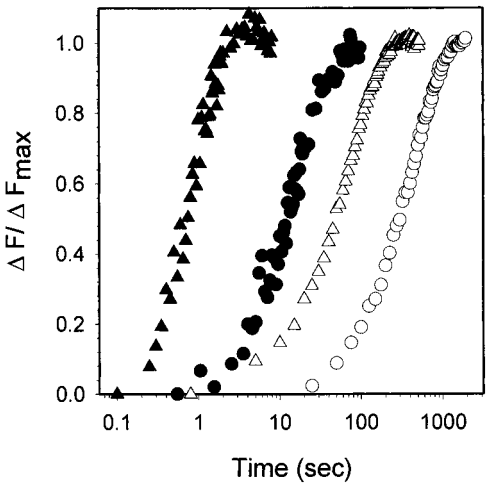

FIGURE 1: Time course of ϵATP incorporation into MgATP−actin (circles) and MgADP−actin (triangles). All samples contained 10 mM MOPS, 0.1 M KCl, 2 mM $MgCl_2$, and 10 μM ϵATP (pH 7.0). MgATP−actin samples contained <1 μM unbound ATP, and MgADP−actin samples contained 3 μM unbound ADP. Samples without profilin (white symbols) contained 0.2 μM Mg−actin. Samples with profilin (black symbols) contained 1.5 μM profilin and 0.5 μM Mg−actin. Data are normalized as the ratio of the fluorescence intensity change to the total fluorescence intensity change ($\Delta F/\Delta F_{max}$).

RESULTS

Effect of Profilin on Actin-Bound Nucleotide Exchange. Figure 1 shows the time course (note the logarithmic time scale) for the exchange of ϵATP for actin-bound ADP or ATP under the physiologically relevant ionic conditions of 0.1 M KCl and 2 mM $MgCl_2$ (pH 7.0). In the absence of profilin, there is a 4-fold lower rate constant for ATP release from MgATP−actin (0.0025 ± 0.0003 s^{-1}, $n = 5$) than for ADP release from MgADP−actin (0.009 ± 0.001 s^{-1}, $n = 4$). Performing similar experiments at pH 8.0, we obtained dissociation rate constants for dissociation of ATP and ADP from MgATP−actin and MgADP−actin of 0.012 and 0.033 s^{-1}, respectively (data not shown). When 1.5 μM profilin is included in the exchange experiments (Figure 1, black symbols), the observed rate constants for nucleotide dissociation increased to 0.06 s^{-1} for MgATP−actin and to 0.8 s^{-1} for MgADP−actin. Figure 2 shows data from experiments similar to those whose data are depicted in Figure 1 in which the observed rate constant, k_{obs}, for nucleotide exchange was determined as a function of the profilin concentration, [P]. Under conditions where the amount of bound profilin can be neglected, these data can be fit by the following equation (*7*):

$$k_{\mathrm{obs}} = (K_{\mathrm{n,p}}k_{-\mathrm{n}} + [\mathrm{P}]k_{-\mathrm{n,p}})/([\mathrm{P}] + K_{\mathrm{n,p}}) \qquad (1)$$

where $K_{n,p}$ is the dissociation constant for the profilin−actin complex, $k_{-n,p}$ is the rate constant for release of nucleotide from the profilin−actin complex, and k_{-n} is the rate constant for release of nucleotide from actin in the absence of profilin.

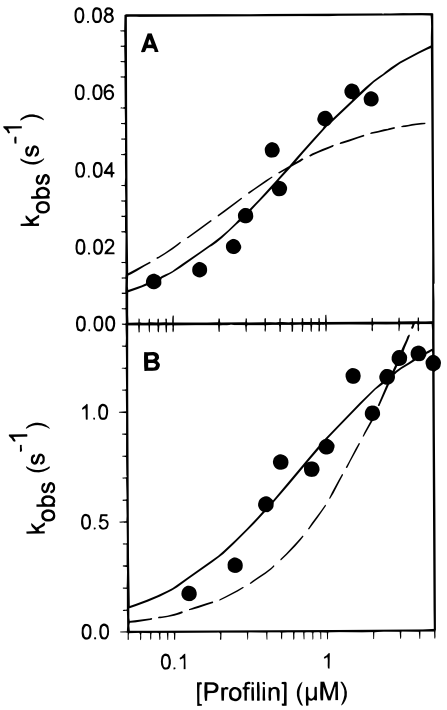

FIGURE 2: Experiments were performed as described in the legend of Figure 1 and the observed rate constants for nucleotide exchange, k_{obs}, determined as a function of the profilin concentration. The solid lines represent fits of eq 1 to the data. (A) $K_{ATP,p} = 0.60$ μM; $k_{-ATP} = 0.0025$ s^{-1}, and $k_{-ATP,p} = 0.080$ s^{-1}. (B) $K_{ADP,P} = 0.65$ μM; $k_{-ADP} = 0.009$ s^{-1}, and $k_{-ADP,p} = 1.45$ s^{-1}. The dashed lines in panels A and B are fits to the hypothesis (*7*) that $K_{ATP,p}/K_{ADP,p} = 20$, by setting $K_{ATP,p}$ equal to 0.2 μM and $K_{ADP,p}$ equal to 4 μM and fitting $k_{-ATP,p}$ and $k_{-ADP,p}$.

Rates of dissociation of ATP and ADP from actin in the absence of profilin (k_{-ATP} and k_{-ADP}, respectively) were fixed at 0.0025 and 0.009 s^{-1}, respectively, and the remaining parameters were derived from the curve fit (Figure 1). The fit (solid line) to the ATP−actin data (●) in Figure 2A results in a $K_{ATP,p}$ of 0.60 ± 0.21 μM and a $k_{-ATP,p}$ of 0.080 ± 0.009 s^{-1}. The fit (solid line) to the ADP−actin data (●) in Figure 2B yields a $K_{ADP,p}$ of 0.65 ± 0.17 μM and a $k_{-ADP,p}$ of 1.45 ± 0.09 s^{-1}. In contrast to the report by Perelroizen et al. (*7*), we find that profilin binds equally well to MgADP−actin and MgATP−actin. Analysis of the data if a 20-fold higher affinity of profilin for ATP−actin than for ADP−actin is assumed (*7*) results in a poor fit to the data; the dashed lines in Figure 2 show the fit using this hypothesis where $K_{ATP,p}$ and $K_{ADP,p}$ values of 0.2 and 4 μM, respectively, were fixed and $k_{-ATP,p}$ and $k_{-ADP,p}$ values of 0.057 and 2.9 s^{-1}, respectively, were obtained from the fit. The most important finding here is that profilin increases the rate constant for dissociation of nucleotide from Mg−actin 25-fold for ATP and 140-fold for ADP.

Effects of Profilin on Actin Polymerization during Sonication. The rate constant for dissociation of ADP from monomeric actin ($k_{-ADP} = 0.009$ s^{-1}) is low enough to impact the turnover of actin during rapid steady state cycling of monomers on and off filaments. One way to induce rapid steady state turnover of subunits within F-actin is to increase the filament number by sonication. The fluorescence intensity of pyrene-labeled actin cannot be used to observe the effects of profilin on actin polymerization during sonication because profilin interacts only weakly with actin labeled at cysteine

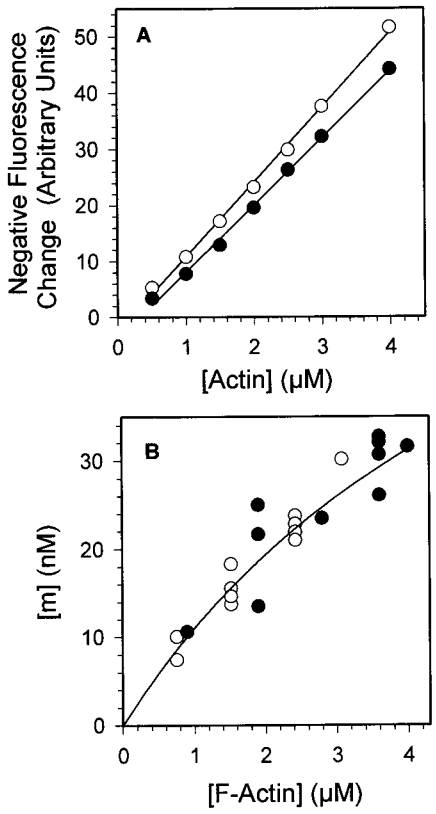

FIGURE 3: (A) Intrinsic fluorescence intensity of actin samples with (●) and without (○) 0.5 μM profilin measured before and after polymerization and plotted as the (negative) change in fluorescence intensity due to polymerization [the intrinsic fluorescence intensity decreases ~30% due to polymer formation (*15*)]. Polymerization was initiated and monitored during sonication as described in Materials and Methods, but measurements of the initial and final fluorescence intensities were made at steady state in the absence of sonication, after any time-dependent fluorescence intensity changes were complete. (B) The filament number concentration generated at steady state during sonication of F-actin was determined in the presence (●) and absence (○) of 0.5 μM profilin. Experimental conditions during sonication were identical to those used in the polymerization experiments whose results are depicted in Figures 4−8, and the assay was accomplished as described in Materials and Methods.

374. Therefore, we have chosen to use actin intrinsic fluorescence to monitor the polymerization of Mg−actin. Figure 3A shows the linear change in tryptophan fluorescence observed for samples with increasing actin concentrations, polymerized in the presence and absence of 0.5 μM profilin. The slight difference in the slopes can be attributed to a decrease in fluorescence intensity that occurs when profilin binds to actin (*16*). These plots are used to convert the fluorescence change to polymer concentration in experiments with and without profilin.

Figure 3B shows the relationship between F-actin concentration and the concentration of filament ends, [m], measured at steady state during sonication. In agreement with previous work, the sonication process yielded filaments which were ~100 subunits in length and the concentration of filament ends at steady state was a predictable function of the steady state polymer concentration (*19*).

Figure 4A shows a typical experiment in which 2.5 μM actin was rapidly polymerized by applying sonication at $t = 0$. During the sonication, a peak in the amount of polymer formed was reached (designated as *a* in Figure 4A), after

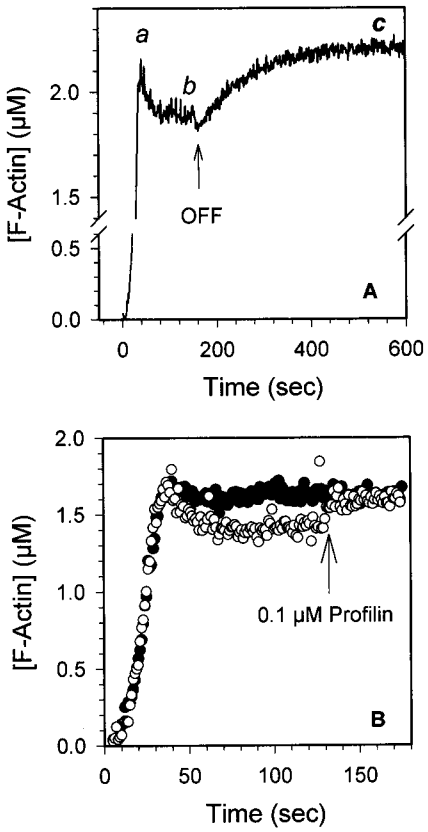

FIGURE 4: (A) Polymerization of 2.5 μM MgATP−actin was initiated by sonication at $t = 0$, monitored by the change in intrinsic fluorescence intensity, and converted to F-actin concentration by a standard curve similar to that of Figure 3A. The ordinate scale has a break so the transient peak in polymer formation designated as *a* and the subsequent decrease in polymer concentration to a plateau designated as *b* could be magnified. Sonication was stopped at the arrow marked OFF, and the increase in the level of F-actin was monitored as it reached a plateau designated as *c*. Experimental conditions are described in Materials and Methods. (B) Polymerization of 2 μM MgATP−actin in the presence (●) and absence (○) of 0.04 μM profilin was initiated by and monitored during sonication as described for panel A. At the arrow, with sonication still being carried out, 0.1 μM profilin was added to the sample without profilin. The effect of profilin addition on the fluorescence was neglected as discussed in Materials and Methods.

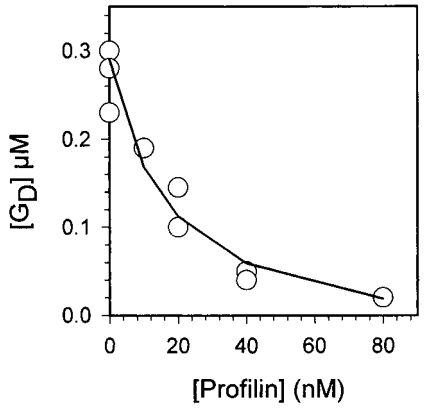

FIGURE 5: Experiments were conducted under the same conditions as described in the legend of Figure 4B except that the concentration of profilin was varied from 0 to 80 nM. [G_D] was calculated from the difference in fluorescence between the intensity peak (Figure 4A, *a*) and the steady state plateau (Figure 4A, *b*) during sonication using a critical concentration plot (without added profilin) similar to Figure 3A. As noted in Materials and Methods, at concentrations below 0.1 μM, fluorescence contributions from profilin and profilin−actin complexes are negligible.

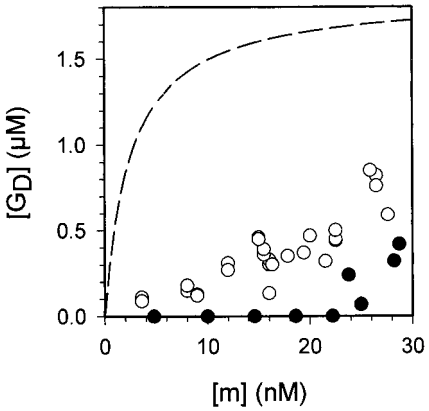

FIGURE 6: Experiments were conducted as described in the legend of Figure 4A, in the presence (●) and absence (○) of 0.5 μM profilin. [G_D] was determined from the change in fluorescence intensity from steady state during sonication (Figure 4A, plateau *b*) to steady state after sonication was stopped (Figure 4A, plateau *c*), using a calibration curve as described in Materials and Methods. The dashed line is the result expected if the increase in [G_D] were calculated using eq 5 (*4*).

which a slow decrease in the amount of polymer to a plateau (*b*) occurred. When the sonication was stopped (arrow), the amount of polymer increased slowly to a new steady state plateau (*c*). Figure 4B shows a similar experiment in which 2 μM Mg−actin was polymerized under sonication in the presence (black symbols) and absence (white symbols) of 0.04 μM profilin. Note that in the sample containing profilin, the peak amount of polymer formed (*a*) is reached and maintained; i.e., there is no decrease to a lower plateau level (*b*) as occurs in the sample without profilin. If 0.1 μM profilin was added (arrow) to this latter sample at plateau *b*, there was a rapid increase in the level of polymer to that of the sample initially containing profilin. The rate of this increase in polymer concentration was much faster than that which occurs on cessation of sonication as shown in Figure 4A. The simplest explanation for these results is that, under sonication, in the absence of profilin, ADP−actin monomer (G_D) accumulates in the solution, as has been observed by Pantaloni et al. (*4*). The absence of an appreciable amount of G_D in the presence of profilin implies that the increased rate of exchange of ATP for ADP on actin reduces the G_D concentration and increases the polymer concentration toward that consistent with an ATP−actin (G_T) critical concentration.

The results of a series of experiments conducted as described for Figure 4B are shown in Figure 5. In these experiments, the G_D concentration was estimated from the difference between the peak amount of polymer (Figure 4A, *a*) and the plateau reached at steady state (Figure 4A, *b*). The ability of 10 nM profilin to reduce the monomer concentration by 50% is a clear demonstration that the potent action of profilin on actin-bound nucleotide exchange affects the steady state actin monomer concentration at the high filament concentrations present during sonication.

Figure 6 shows the G_D concentration calculated as the change in polymer concentration which occurs after terminating sonication (Figure 4A, plateau *c* minus plateau *b*) for a number of experiments at various filament end concentrations. Here we determined the G_D concentration in a manner

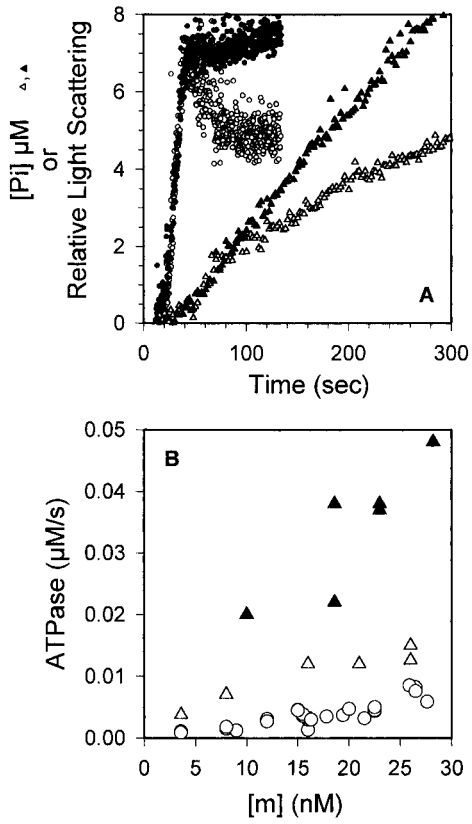

FIGURE 7: (A) Polymerization was initiated under continuous sonication in a 2 μM MgATP−actin sample in the absence (white symbols) and presence (black symbols) of 0.5 μM profilin. The light scattering intensity at 90° (circles), reflecting polymer formation, and the extent of absorption (triangles), for measuring the release of inorganic phosphate, were monitored simultaneously. Experimental details are described in Materials and Methods. (B) The rate of release of inorganic phosphate at steady state (ATPase) was monitored as described for panel A at various filament end concentrations in the presence (▲) and absence (△) of 0.5 μM profilin. The open circles are ATPase rates predicted by calculation using eq 3, with [G_D] values from Figure 4A (○) and a k_{-ADP} of 0.01 s^{-1}.

different from that used in the experiments of Figure 5 because at filament end concentrations of >20 nM the polymerization peak (*a*) is attenuated by the onset of the depolymerization reaction. In the absence of profilin (○), the G_D concentration increases with filament number concentration, but the presence of 0.5 μM profilin prevents this increase at filament end concentrations below 20 nM.

The ATP−actin monomer concentration ([G_T]), in the absence of profilin, could be calculated from the mass equation

$$[G_T] = [\text{actin}]_{\text{total}} - [\text{F-actin}] - [G_D] \qquad (2)$$

These measurements were noisy, and the combined data (not shown) yielded an average [G_T] of 0.1 ± 0.1 μM (n = 22), and we could detect no apparent dependence on filament concentration over the range of 4−30 nM.

ATP Hydrolysis and Actin Turnover during F-Actin Sonication. Figure 7A shows results from an experiment in which 2 μM MgATP−actin was polymerized under sonication in the presence (black symbols) and absence (white symbols) of 0.5 μM profilin. In this experiment, we measured the rate of release of P_i (circles) from the polymer using the spectrophotometric assay of Webb (*18*), while simultaneously monitoring the rate of polymer formation using 90° light scattering measurements (triangles). Light scattering was used because the wavelength of light required for the P_i assay (360 nm) was too high to excite actin intrinsic fluorescence. The measurements clearly demonstrate that polymer formation is nearly complete before release of P_i begins. As the rate of P_i release becomes maximal, indicating rapid formation of ADP−actin polymer, the sample without profilin begins to depolymerize. After about 2 μM P_i has been released, the rate of P_i release slows, reflecting a lower steady state ATPase rate. Compared to the sample without profilin, the sample with profilin polymerizes to the same peak polymer concentration, but remains at this level and does not undergo the subsequent partial depolymerization phase. Also, with profilin present, no deceleration in the P_i release rate occurs; instead, ATP hydrolysis continues at a constant rate. Figure 7B shows the results of a series of experiments in which the rate of ATPase was measured during steady state sonication of F-actin with (▲) and without (△) 0.5 μM profilin. In the absence of profilin, the steady state ATPase rate that occurs after polymerization is complete can be related to the G_D concentration by

$$\text{ATPase rate} = k_{-ADP}[G_D] \qquad (3)$$

The measured steady state ATPase rate in the absence of profilin appears to be approaching a plateau consistent with a k_{-ADP} of 0.01 s^{-1} and a [G_D] of ≈1.5 μM. ATPase rates measured in the presence of profilin were significantly higher and linearly related to [m], suggesting that [G_T] is maintained in the presence of profilin. In the presence of profilin

$$\text{ATPase rate} = k_{-ADP}[G_D] + k_{-ADP,p}[PG_D] \qquad (4)$$

where [PG_D] is the concentration of profilin complexed with G_D, k_{-ADP} = 0.01 s^{-1}, and $k_{-ADP,p}$ = 1.4 s^{-1} is the rate constant for ADP dissociation from PG_D. Using data from Figures 6 and 7B, we estimate that [PG_D] < 30 nM for [m] up to 30 nM. [PG_D] is kept low by rapid conversion to PG_T (profilin−G_T complex), effectively renewing the G_T pool and maintaining a maximal ATPase activity.

Measurements of the G_D concentration (Figure 6) as a function of [m] in the absence of profilin can be used to estimate the ATP hydrolysis rates during sonication of F-actin. The open circles in Figure 7B show these calculated values. These values are somewhat lower than the measured values. We are not sure why this is so; it is possible that we have underestimated the G_D concentration; alternatively, it may be that the rate constant, k_{-ADP}, is increased by sonication, or that there is some ATP hydrolysis which occurs along the length of the filament independent of G_T monomer addition to the filament end. The difference is not large, and could be the result of a combination of contributing factors.

DISCUSSION

Nucleotide Exchange at Physiological Ionic Strength. The measurements of the rate of nucleotide release from monomeric actin at physiological ionic strength and pH 7.0 presented here are comparable with results from previous studies (*7*, *9*). Increasing the ionic strength with 0.1 M KCl

and 2 mM $MgCl_2$ results in an increase in the ATP dissociation rate constant from 0.0005 to 0.0025 s^{-1} and an increase in the ADP dissociation rate constant from 0.003 to 0.009 s^{-1}. Significantly, the values for both rate constants under physiological ionic conditions are about 20-fold smaller than those reported for the ATP analogues ϵADP and ϵATP at pH 8.0 (*7*). Our value for k_{-ADP} is, however, in good agreement with the value of 0.007 s^{-1} recently reported by Teubner and Wegner (*21*). It has been previously documented (*7*), and we have confirmed, that increasing the pH from 7.0 to 8.0 increases the dissociation rate constants for nucleotide release from monomeric actin 3−5-fold. We suspect that the intrinsically weaker binding of the ϵ-nucleotide analogues to actin, particularly at pH 8.0, accounts for the differences between our data and those of Perelroizen et al. (*7*). The important point to be made is that release of ADP from MgADP−actin is relatively slow under physiological conditions.

Measurements of Actin Polymerization during Sonication. The effects of monomer actin cycling and nucleotide exchange on F-actin dynamics in vivo are likely to be complicated by a variety of factors. The activity of actin-binding proteins, the number and subunit composition of the actin filaments, and compartmentalization of energy stores are all likely to impact F-actin dynamics. The mechanistic details of the actin depolymerization reaction, the impact of nucleotide exchange at the ends of actin filaments (*21*), and the mechanisms by which the ADP−actin monomer is generated during actin filament turnover within cells are not fully understood. The experimental approach presented here may improve our understanding of the basic elements of the system.

The use of actin intrinsic fluorescence to monitor polymerization is important in eliminating bias introduced by labeling of actin. Although the signal change upon polymerization is only ~30%, we show in Figure 3A that data of good quality can be obtained. Our estimates of the steady state concentrations of the actin monomer and polymer during and after sonication depend on accurate measurements of the fluorescence intensity difference between the two steady states. The sonication process increases noise, and in some cases, baseline shifts in fluorescence intensity occur on starting or stopping sonication. These small baseline shifts were easily accounted for in our measurements; noise was more of a problem. Since estimates of the G_T concentration are derived from measurements made during sonication, and are calculated as a small difference between large numbers, they are more unreliable than our estimates of the G_D concentration.

Finally, the measurements of the filament concentrations proved to be fairly reproducible. In developing the assay, we incidentally learned some interesting facts about our sonication system. We found that changing the sample volume, the insertion depth of the sonicator tip, or the power applied caused no detectable change in the steady state filament concentration. The primary determinant of filament concentration during sonication appears to be the F-actin concentration. This result was in excellent agreement with our previous study (*19*), in which we found that, during sonication, filaments are fragmented to a constant length of about 100 subunits.

In most in vitro polymerization experiments, where the filament number concentration is <1 nM and the barbed ends contain predominantly ATP−actin, significant concentrations of monomeric ADP−actin are not present. The description of actin polymerization during sonication described here may be more applicable to the in vivo scenario where the filament number concentration is regulated by capping and severing proteins. Most (but possibly not all) of the proteins that sever also cap the barbed filament end after severing. These caps can be released by polyphosphoinositides, thus permitting ADP−actin monomer dissociation. In these cases, a protein such as profilin, which increases the exchangeability of actin-bound nucleotide, may be important in maintaining the ATP−actin monomer concentration to promote cycling of actin monomers.

Actin Polymerization during Sonication. Shifts in monomer concentration during sonication, with accumulation of ADP−actin (G_D), were first described by Pantaloni et al. (*4*) using the following equation:

$$[G_D] = k_4[m]/(k_{-ADP} + k_3[m]) \quad (5)$$

where k_3 and k_4 are the forward and reverse rate constants, respectively, for addition of G_D to polymer ends, m, and k_{-ADP} is effectively the rate constant for exchange of actin-bound ADP for ATP under conditions of high ATP:ADP ratios.

The dashed line in Figure 6 shows the results predicted by eq *5* and clearly does not describe our experimental data; its shortcoming results from the uncoupling of ATP hydrolysis from the actin filament elongation reaction.

A steady state model which describes the relationship between [m], $[G_T]$, and $[G_D]$, and which better reflects the experimental results, is developed here. The differential equations describing polymerization of G_T and G_D can be written as

$$d[G_T]/dt = k_2[m_t] - k_1[G_T][m] + k_{-ADP}[G_D] \quad (6)$$

$$d[G_D]/dt = k_4[m_d] - k_3[G_D][m] - k_{-ADP}[G_D] \quad (7)$$

where $[m_t]$ and $[m_d]$ are the concentrations of filament ends with terminal subunits containing ATP and ADP, respectively, k_1 and k_3 are association rate constants and k_2 and k_4 are dissociation rate constants for G_T and G_D, respectively, and k_{-ADP} is the rate constant for dissociation of ADP from G_D. These equations state that G_T and G_D can dissociate only from ends, m_t and m_d, which contain the appropriate terminal subunits. A simple calculation[2] shows that the nucleotide composition of filament ends is defined predominantly by

[2] At steady state, the rate of filament fragmentation equals the rate of filament annealing, and the published annealing rate constant of k_a (2.2 μM^{-1} s^{-1}; *19*) can be used to calculate the fragmentation rate $k_a[m]^2$. The ratio of add-on events to fragmentation (and annealing) events is $(k_1[G_T] + k_3[G_D])/k_a[m]$. When $k_1 = 12$ μM^{-1} s^{-1}, $k_3 = 4$ μM^{-1} s^{-1}, $[G_T] = 0.1$ μM, and the $[G_D]$ from Figure 6 is used, then for $[m] = 4-30$ nM this ratio is >50 so that the nucleotide composition of the filament ends is predominantly determined by monomer add-on reactions, as was pointed out by one of the reviewers. Similarly, filament ends with subunits containing ADP−P_i, produced by ATP hydrolysis at an m_t end, would occur at the hydrolysis rate of 0.1 s^{-1} (*20*), much slower than the filament elongation rate ($k_1[G_T] + k_3[G_D]$). This assumption may not be correct for the (less kinetically active) pointed ends, but our analysis is concerned primarily with the barbed ends.

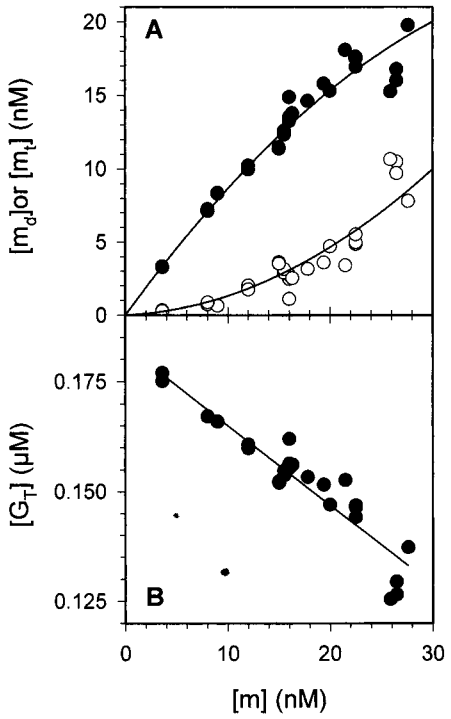

FIGURE 8: (A) Concentrations of filament ends containing terminal ADP−actin subunits, $[m_d]$ (○), and terminal ATP−actin subunits, $[m_t]$ (●), were calculated from eqs 10 and 11, respectively, using the $[G_D]$ data measured during steady state sonication in the absence of profilin and shown in Figure 6 (○). The following parameters were used in the calculation: $k_3 = 4\ \mu M^{-1}\ s^{-1}$, $k_4 = 7\ s^{-1}$, and $k_{-ADP} = 0.01\ s^{-1}$. (B) $[G_T]$ was calculated from eq 9 as a function of filament end concentration using $[m_t]$ values from panel A and $[G_D]$ values from Figure 6. The following parameters were used in the calculation: $k_1 = 12\ \mu M^{-1}\ s^{-1}$, $k_2 = 2\ s^{-1}$, and $k_{-ADP} = 0.01\ s^{-1}$.

monomer add-on reactions rather than through exposure of internal subunits by fragmentation during sonication, or by hydrolysis of ATP on terminal subunits. Thus, we neglect the possibility that a filament may have a terminal subunit containing ADP−P_i and consider only the two types of filament ends, m_t and m_d.

At steady state, when $d[G_T]/dt = d[G_D]/dt = 0$, eqs 6 and 7 yield

$$[G_D] = k_4[m_d]/(k_{-ADP} + k_3[m]) \quad (8)$$

$$[G_T] = (k_2[m_t] + [G_D]k_{-ADP})/k_1[m] \quad (9)$$

Note that eq 8 differs from eq 5 in that $k_4[m]$ is replaced by $k_4[m_d]$, but $k_3[m]$ is the same in both equations.

Equation 8 can be rearranged to

$$[m_d] = [G_D](k_{-ADP} + k_3[m])/k_4 \quad (10)$$

Then $[m_t]$ is

$$[m_t] = [m] - [m_d] \quad (11)$$

Figure 8A shows $[m_d]$ and $[m_t]$ as functions of [m], calculated from the $[G_D]$ data in Figure 6. In the absence of profilin, the increase in $[G_D]$ with increasing filament number results in an approximately parabolic increase in $[m_d]$ over the filament concentration range of 0−30 nM. Thus, the relative concentration of m_d ends, $[m_d]/[m]$, increases with increasing [m], and the relative concentration of m_t ends decreases with increasing [m].

Calculation of $[G_T]$ from eq 9, using values of $[m_t]$ from Figure 8A, predicts a decrease in $[G_T]$ from 0.18 to 0.13 μM as [m] increases from 4 to 30 nM. These values are within the range of our experimental estimates of $[G_T]$, but the decrease with filament number concentration would not be detectable above the noise of our experimental measurements of $[G_T]$.

In the presence of profilin, k_{-ADP} can be increased from 0.01 to 1.4 s^{-1}. Equation 8 predicts that as k_{-ADP} increases, $[G_D]$ decreases. Consistent with this prediction, in the presence of profilin, when [m] < 20 nM, an increase in $[G_D]$ was not observed (Figure 6). When [m] > 20 nM, an increase in $[G_D]$ was observed, indicating that the low profilin concentration used in these experiments was not enough to convert the entire G_D monomer population into G_T and PG_T at steady state. We do not attempt to include profilin−actin complexes, PG_D and PG_T, in the analysis. The steady state concentrations of these complexes depend on as yet undetermined parameters, such as their respective polymerization rate constants, as well as on the actin binding affinities and the nucleotide exchange rate constants determined in this study.

Effects of Profilin on Actin-Bound Nucleotide Exchange and Actin Polymerization. An important finding of this study is that profilin binds with a similar affinity to ATP−actin and ADP−actin. Vinson et al. (*22*), using actin and profilin from *Acanthamoeba*, reported a 5−8-fold difference in affinity, while Perelroizen et al. (*7*), using the same proteins that were used here, reported a 20-fold difference. The difference between our data and theirs can most likely be attributed to weaker binding of profilin to ϵADP−actin than to ADP−actin, differences in experimental conditions, such as pH, and differences in protein sources. At physiological ionic strength, monomeric actin binds ATP with an affinity 3-fold higher than for ADP (*23*). However, the profilin−actin complex binds ATP 18-fold better than ADP (assuming the association rate constants for ATP and ADP binding to the complex are equal). If the ATP:ADP concentration ratio in a cellular compartment were to decrease to 1, the ATP−actin:ADP−actin concentration ratio would be 3 in the absence of profilin, and would increase to 18 in the presence of a saturating level of profilin. The 140-fold increase in the rate of release of ADP from MgADP−actin on binding of profilin ensures rapid formation of MgATP−actin during high fluxes of ADP−actin monomers.

The results of the ATPase measurements depicted in Figure 7B demonstrate the ability of profilin to increase the concentration of ATP−actin at steady state during sonication. If the profilin−ATP−actin complex (PG_T) has polymerization characteristics similar to those of G_T, then the roughly 2-fold increase in the rate of ATPase caused by addition 0.5 μM profilin indicates an increase in the steady state flux of G_T due to an increase in the effective k_{-ADP}. As shown in Figure 8B, in the absence of profilin, $[G_T]$ decreases with increasing m concentrations; the increase in k_{-ADP} caused by profilin suppresses this decrease by increasing the extent of G_T regeneration. Given that the filament length during sonication is approximately constant (~100 subunits), this increased supply of G_T translates into an increase in the amounts of F-ATP−actin and F-ADP−P_i−actin subunits

within the polymer. The understanding that actin filaments are composed of subunits with differing nucleotide compositions (ATP, ADP−P_i, and ADP) has generated interest in the possibility that proteins which bind to F-actin are able to differentiate between the various subunits. Actin depolymerizing factor (cofilin/ADF), for example, is thought to bind only to subunits containing ADP−actin (*24*), and may cause disruption and severing of the filament (*25*). Similarly, the extent of F-actin severing by gelsolin is found to be increased in filaments composed predominantly of ADP−actin subunits (*26*). An important function of profilin may be to ensure that actin filaments are continuously charged with ATP−actin subunits. Since this effect will predominate at the more kinetically active barbed end of the filament, it may "protect" the barbed end region from the action of severing proteins and leave the pointed end region more vulnerable to their actions.

Is Enhancement of Nucleotide Exchange by Profilin Physiologically Important? The answer to this question is controversial. Perelroizen et al. (*8*) have shown that profilin from plants does not increase the rate of nucleotide exchange on muscle actin. However, plant profilin binds to muscle actin with a very low affinity. The affinity of profilin binding to actin is likely to affect the binding of nucleotide to the profilin−actin complex; profilin which binds weakly may not provide the binding energy necessary to induce the conformational changes leading to an increased level of nucleotide exchange. In this study, we have used the well-characterized skeletal muscle α-actin isoform. It will be important to characterize the effects of profilin on the nonmuscle isoforms of actin, which are reported to bind profilin with a higher affinity than skeletal muscle actin (*27*). As we have shown here, nucleotide exchange affects actin polymerization dynamics at high concentrations of filament ends. Studies of the interactions of plant and animal profilins and actins at high filament number will further define the importance of increased actin-bound nucleotide exchange by profilin.

Perelroizen et al. (*8*) have proposed that the major function of profilin is to use the energy of ATP hydrolysis to establish directionality of filament growth and lower the critical concentration of ATP−actin. Our results support this concept, but indicate a different mechanism than they suggest. Our data do not directly address the effects of profilin on $[G_T]$, but suggest that by keeping $[G_D]$ low, profilin ensures that the filament maintains a composition of F-ATP−actin and F-ADP−P_i−actin subunits at the growing end. The resultant absence of F-ADP−actin subunits at the growing end allows proper functioning of the so-called "phosphate timer" which may be used by actin binding proteins to distinguish between newly polymerized and older subunits within a filament, i.e., to distinguish between the growing barbed end and the older pointed end. This interpretation may help to explain the recent report that profilin is required for timing of actin polymerization in response to thermal stress (*28*).

Ultimately, the physiological relevance of nucleotide exchange on actin largely depends on other actin-binding proteins. As pointed out by Zigmond (*29*), the rate of actin turnover within cells is at least 1 order of magnitude higher than in vitro measurements suggest. If the in vivo rates of actin ATP hydrolysis and P_i release are similar to those presented here, then slow P_i release limits the actin "aging" process and ultimately limits actin turnover. There may be proteins, not yet discovered, which alter the P_i release rate and thus would change this limit. The ADF/cofilin family of proteins, which bind to F-ADP− and G-ADP−actin, are likely to be key proteins in actin dynamics, and they apparently use phosphate release to time their interaction with F-actin, increase the depolymerization rate, and perhaps sever the filament (*23*, *30*). Our experimental approach has allowed a description of the effects of profilin on actin polymerization and should help to answer key questions concerning actin filament dynamics in the presence of other actin-binding proteins.

ACKNOWLEDGMENT

We thank Dr. Jay Newman and Dr. Paul Higgins for critical reading of the manuscript and the anonymous reviewers for a thorough and helpful review.

REFERENCES

1. Cooper, J. A. (1991) *Annu. Rev. Physiol. 53*, 585−605.
2. Theriot, J. A., and Mitchison, T. J. (1991) *Nature 352*, 126−131.
3. Theriot, J. A., Mitchison, T. J., Tilney, L. G., and Portnoy, D. A. (1992) *Nature 357*, 257−260.
4. Pantaloni, D., Carlier, M.-F., Coué, M., Lal, A. A., Brenner, S. L., and Korn, E. D. (1984) *J. Biol. Chem. 259*, 6274−6283.
5. Pring, M., Weber, A., and Bubb, M. R. (1992) *Biochemistry 31*, 1827−1836.
6. Goldschmidt-Clermont, P. J., Machesky, L. M., Doberstein, S. K., and Pollard, T. D. (1991) *J. Cell Biol. 113*, 1081−1089.
7. Perelroizen, I., Carlier, M.-F., and Pantaloni, D. (1995) *J. Biol. Chem. 270*, 1501−1508.
8. Perelroizen, I., Didry, D., Christensen, H., Chue, N. H., and Carlier, M.-F. (1996) *J. Biol. Chem. 271*, 12302−12309.
9. Kinosian, H. J., Selden, L. A., Estes, J. E., and Gershman, L. C. (1993) *J. Biol. Chem. 268*, 8683−8691.
10. Selden, L. A., Estes, J. E., and Gershman, L. C. (1989) *J. Biol. Chem. 264*, 9271−9277.
11. Kinosian, H. J., Selden, L. A., Estes, J. E., and Gershman, L. C. (1996) *Biochemistry 35*, 16550−16556.
12. Lindberg, U., Schutt, C. E., Hellsten, E., Tjader, A.-C., and Hult, T. (1988) *Biochim. Biophys. Acta 967*, 391−400.
13. Kaiser, D. A., Goldschmidt-Clermont, P. J., Levine, B. A., and Pollard, T. D. (1989) *Cell Motil. Cytoskeleton 14*, 251−262.
14. Gershman, L. C., Selden, L. A., Kinosian, H. J., and Estes, J. E. (1989) *Biochim. Biophys. Acta 995*, 109−115.
15. Selden, L. A., Kinosian, H., Estes, J. E., and Gershman, L. C. (1994) *Adv. Exp. Med. Biol. 358*, 51−57.
16. Perelroizen, I., Marchand, J.-B., Blanchoin, L., Didry, D., and Carlier, M.-F. (1994) *Biochemistry 33*, 8472−8478.
17. Pollard, T. D. (1986) *J. Cell Biol. 103*, 2747−2754.
18. Webb, M. R. (1992) *Proc. Natl. Acad. Sci. U.S.A. 89*, 4884−4887.
19. Kinosian, H. J., Selden, L. A., Estes, J. E., and Gershman, L. C. (1993) *Biochemistry 32*, 12353−12357.
20. Pollard, T. D., and Weeds, A. G. (1984) *FEBS Lett. 170*, 94−98.
21. Teubner, A., and Wegner, A (1998) *Biochemistry 37*, 7532−7538.
22. Vinson, V. K., De La Cruz, E. M., Higgs, H. N., and Pollard, T. D. (1998) *Biochemistry 37*, 10871−10880.
23. Wanger, M., and Wegner, A. (1993) *Biochim. Biophys. Acta 914*, 112−116.
24. Maciver, S. K., Zot, H. G., and Pollard, T. D. (1991) *J. Cell Biol. 115*, 1611−1620.

25. Cooper, J. A., Blum, J. D., Williams, R. C., and Pollard, T. D. (1986) *J. Biol. Chem. 261*, 477−485.
26. Allen, P. G., Laham, L. E., Way, M., and Janmey, P. A. (1996) *J. Biol. Chem. 271*, 4665−4670.
27. Larsson, L., and Lindberg, U. (1988) *Biochim. Biophys. Acta 153*, 95−105.
28. Yeh, J., and Haarer, B. K. (1996) *FEBS Lett. 398*, 303−307.
29. Zigmond, S. H. (1993) *Cell Motil. Cytoskeleton 25*, 309−316.
30. Carlier, M.-F., Laurent, V., Santolini, J., Melki, R., Didry, D., Xia, G.-X., Hong, Y., Chua, N.-H., and Pantaloni, D. (1997) *J. Cell Biol. 136*, 1307−1323.

BI981543C